

## Screening of hydrodynamic interactions for polyelectrolytes in salt solution

Jens Smiatek, Friederike Schmid

Condensed Matter Theory Group, Fakultät für Physik, Universität Bielefeld

(Dated: September 30, 2008)

We provide numerical evidence that hydrodynamic interactions are screened for charged polymers in salt solution on time scales below the Zimm time. At very short times, a crossover to hydrodynamic behavior is observed. Our conclusions are drawn from extensive coarse-grained computer simulations of polyelectrolytes in explicit solvent and explicit salt, and discussed in terms of analytical arguments based on the Debye-Hückel approximation.

PACS numbers: 82.35.Rs, 47.57.jl, 87.15.A-

Macromolecules of biological relevance such as DNA are often highly charged polyelectrolytes. Under physiological conditions, these molecules are dissolved in salt solutions with Debye lengths of less than 1 nm. From the point of view of statics, the electrostatic interactions are thus screened: Large DNA strands in physiological buffers have similar static properties than regular self-avoiding chains with short range interactions. The dynamical properties are more complex. For neutral chains, solvent-mediated hydrodynamic interactions influence the mobility and the internal modes of the molecules. The signature of these hydrodynamic interactions is dynamical Zimm scaling<sup>1</sup>. For example, the mobility and the diffusion constant  $D$  of a self-avoiding Zimm chain scale as  $D \propto N^{-1}$  with the chain length  $N$ , where  $\nu = 0.588$  is the well-known Flory exponent. In contrast, the same quantities scale as  $N^{-1}$  in a Rouse chain, where hydrodynamic interactions are absent or screened.

For polyelectrolytes like DNA, the interaction with the counterions and salt ions complicates the situation. The polyelectrolyte chain is surrounded by an oppositely charged ion cloud, which drags behind and generates additional friction<sup>2</sup>. This "relaxation effect" reduces their mobility, but the dominating behavior for large chain lengths is still predicted to be Zimm-like, and indeed, the scaling exponents reported in experiments (e.g.,  $D \propto N^{0.67}$  for double stranded DNA in Ref. 3) are closer to the Zimm than to the Rouse exponent.

On the other hand, it has long been known that the electrophoretic mobility in an applied electrical field scales like  $\mu_e \propto N^{-1}$  for long chains, i.e., it exhibits Rouse-like behavior<sup>4</sup>. The physical explanation for this effect is rather intuitive: The electrical field acts both on the polyelectrolyte and the surrounding ion cloud. The net momentum transferred to the solvent by all particles is thus zero, and the hydrodynamic interactions are screened as a result. One can derive a screened Oseen tensor, which describes hydrodynamic interactions between monomers in a homogeneous electrical field<sup>2,4</sup>.

Hence it appears that electrostatic and hydrodynamic screening are closely related to each other, and that electrostatic screening may entail hydrodynamic screening if the dynamics is driven by electrical fields. Electrostatic forces drive electrophoresis, but also to some extent the

internal motion of polyelectrolytes, since they dominate the nonbonded interactions between monomers. The question thus arises whether hydrodynamic screening can also be observed in the absence of external fields.

This question is addressed in the present letter. We consider a polyelectrolyte in salt solution, without external fields, and study the dynamics of internal motions in the chain. The dynamical scaling (Zimm vs. Rouse) gives us information on the influence of hydrodynamic interactions. We use a generic coarse-grained model both for the polyelectrolyte and the solvent. Recently, it has been shown that such models can account quantitatively for the dynamics of real polyelectrolytes in solution<sup>5,6</sup>.

On general grounds, we already know that the dynamics on very large time scales, where chain diffusion dominates, must be Zimm-like: By virtue of the Einstein relation, the diffusion constant is related to the mobility of the chain in a sedimentation field, which acts only on the monomers and not on the ions. The interaction between monomers and ions leads to a relaxation effect, as discussed above, but not to hydrodynamic screening. Diffusion-dominated behavior sets in at the "Zimm time", i.e., the time scale on which single monomers follow the center of the mass motion of the whole chain. In the present work, we thus focus on time scales below the Zimm time, where the dynamics is governed by the internal modes of the chain.

We study the dynamics of single bead-spring chains immersed in a solution of solvent particles and ions (salt ions and counterions) by dissipative particle dynamics (DPD) simulations<sup>7</sup>. Ions and monomers are hard-core particles with diameter  $\sigma$ , which interact with the potential  $V_{hc} = 4 \left( \left( \frac{\sigma}{r} \right)^{12} - \left( \frac{\sigma}{r} \right)^6 \right)$  at  $r < \sigma$ . In addition, the ions and a fraction of the monomers carry single-valued charges  $q_e$  and interact via Coulomb potentials. The monomers in the chain are connected by finitely extensible nonlinear elastic (FENE) springs with the bond potential  $V_{bond} = \frac{1}{2} k R^2 \ln(1 - (r/R)^2)$ . The solvent particles provide the fluid background and have no conservative interactions. All particles interact with dissipative DPD forces, which have the usual form<sup>7</sup>  $\mathbf{F}_{ij}^{DPD} = \mathbf{F}_{ij}^D + \mathbf{F}_{ij}^R$  with a viscous contribution  $\mathbf{F}_{ij}^D = \frac{\gamma}{2} \frac{(\mathbf{r}_{ij} \cdot \mathbf{r}_{ij})}{r_{ij}^3} (\mathbf{r}_{ij} \cdot \mathbf{v}_{ij}) \mathbf{r}_{ij}$  and a random force  $\mathbf{F}_{ij}^R = \sqrt{\frac{\gamma}{2} k_B T} \mathbf{r}_{ij} \cdot \mathbf{r}_{ij} \mathbf{r}_{ij}$ . Here  $\mathbf{v}_{ij}$  is the velocity difference

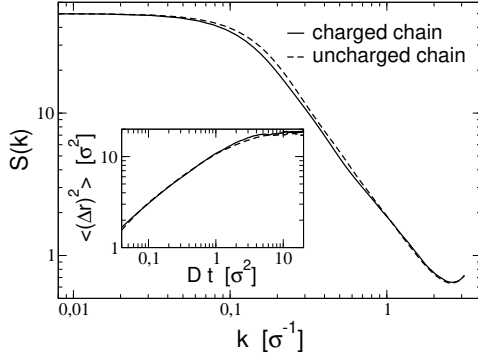


FIG. 1: Static structure factor  $S(k)$  of the charged chain in salt solution (solid line) compared to that of an uncharged chain (dashed line). The inset shows the mean square displacement of the central monomer relative to the center of mass of the chain  $\langle h(r)^2_i \rangle$  as a function of the rescaled time  $Dt$  with the diffusion constant  $D$ .

and  $r_{ij}$  the distance between the two particles  $i$  and  $j$ ,  $\hat{r}_{ij} = r_{ij}/r_{ij}$ ,  $\delta(r) = 1$  ( $= 0$ ) for  $r < 0$  ( $> 0$ ), and  $\delta(r)$  is a Gaussian distributed white noise with mean zero and variance one. All particles have the same mass  $m$ . The natural units in our system are thus the length  $\sigma$ , the thermal energy  $k_B T$ , and the time unit  $\tau_m = \sigma^2 / k_B T$ .

Specifically, we consider chains of length  $N = 50$  with charges on every second monomer, in solutions with ion concentration  $\rho_i = 0.1 \sigma^{-3}$ . The other model parameters are  $e = \sqrt{k_B T}$ ,  $\epsilon = k_B T$ ,  $R = 1.5$ ,  $k = 25 k_B T = \sigma^2$ , and  $\rho_s = 5 k_B T = \sigma^2$ , and the density of solvent particles is  $\rho_s = 3 \sigma^{-3}$ . With these parameters, the motion of the ions in solution is diffusive after an initial ballistic regime of length  $\sigma$ . The Debye length in the solution is  $\lambda_D = 0.89 \sigma$ , the kinematic viscosity of the fluid is  $\eta = 1.24 k_B T = \sigma^3$ , and the ions have the mobility  $\mu = 0.44 \sigma^2 = k_B T$ . The mean radius of uncharged chains of length  $N = 50$  is  $R_{g,u} = 4.74 \sigma$ , and they diffuse with the diffusion constant  $D_u = 0.021 \sigma^2$ . In comparison, the charged chains are just slightly more swollen,  $R_{g,c} = 5.35 \sigma$ , but their diffusion constant is significantly reduced due to the relaxation effect,  $D_c = 0.013 \sigma^2$ . The simulations were carried out in cubic simulation boxes with system size  $L = 25 \sigma$  and periodic boundary conditions, using the time step  $\tau = 0.01 \tau_m$ . The run lengths were 4 million time steps after an equilibration time of 2 million steps.

Fig. 1 compares the static structure factor for such a charged chain in salt solution to that of an uncharged chain with the same length. The charged chain is slightly stretched, otherwise the two structure factors are very similar. A algebraic scaling behavior  $S(k) \sim k^{-\alpha}$  is observed in the wavevector range  $1/R_g < k < 1/a_0$ , where  $a_0 = 1.7 \sigma$  is the distance between charged monomers in the chain. The value of  $\alpha$  is found to be  $\alpha = 0.67$  for the uncharged chain, and  $\alpha = 0.7$  for the charged chain. These values are larger than the universal asymptotic value,  $\alpha = 0.588$ , due to the finite length of the chains.

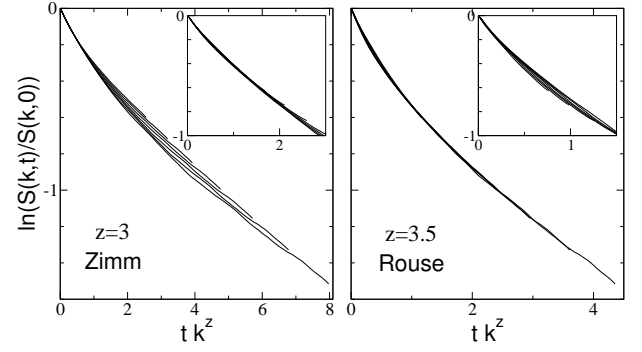


FIG. 2: Dynamic structure factor of the charged chain scaled with Zimm (left) and Rouse (right) exponent  $z$  for wavevectors in the range  $0.2 < k < 0.3$  (large wavelengths) and times  $t < t_{zimm}$ . The inset shows the corresponding data for the uncharged chain.

The inset of Fig. 1 shows the mean square displacement of the central monomer in the reference frame of the chain,  $\langle h(r)^2_i \rangle = \langle h(r_i(t) - R_{cm}(t) - r_i(0) + R_{cm}(0))^2 \rangle$ , as a function of time for charged and uncharged chains. If the time is scaled with the diffusion constant  $D$ , the two curves lie almost on top of each other, indicating that internal modes are slowed down by the relaxation effect in the same way than the overall chain diffusion. The quantity  $\langle h(r)^2_i \rangle$  reaches a plateau at the Zimm time  $t_{zimm}$ . From Fig. 1, we infer  $D t_{zimm} \sim 4 \sigma^2$ , in rough agreement with the heuristic estimate  $6D t_{zimm} \sim R_g^2$ . This yields  $t_{zimm} \sim 300$  for the charged chain, and  $t_{zimm} \sim 200$  for the uncharged chain.

To assess the dynamical properties of the chains, we study the dynamic structure factor  $S(k;t)$ . In the dynamical scaling regime<sup>1,9</sup>, it should exhibit the universal scaling behavior  $S(k;t) = S(k;0)f(tk^z)$  with the exponent  $z = 3$  for Zimm chains and  $z = 2 + 1/\nu$  for Rouse chains. Hence the curves  $S(k;t)/S(k;0)$  for different  $k$  vectors should collapse onto a single master curve  $f(tk^z)$  when plotted against  $tk^z$  with the correct exponent  $z$ . Fig. 2 shows such scaling plots for large wavelengths,  $1/R_g < k < 0.3 \sigma^{-1}$ , using  $\nu = 0.67$ . Not surprisingly, uncharged chains exhibit Zimm scaling. For charged chains, however, the data collapse much better in the Rouse scaling plot than in the Zimm scaling plot: Below the Zimm time, the chain behaves as if hydrodynamic interactions were absent.

A closer inspection of Fig. 2 shows that this is not yet the full story. At very early times, the data collapse in the Zimm plot seem more convincing than in the Rouse plot. Indeed, we can identify a second characteristic time  $t_0 \sim 55$ , below which the data show Zimm scaling for a range of  $k$ -vectors that includes both long and shorter length scales,  $1/R_g < k < 0.5 \sigma^{-1}$  (Fig. 3). For  $t > t_0$ , the Zimm scaling breaks down for all  $k$ . For  $k < k_0 \sim 0.3 \sigma^{-1}$ , one has a crossover to Rouse scaling. For  $k > k_0$ , the data do not scale at all.

To summarize, we find that hydrodynamic interac-

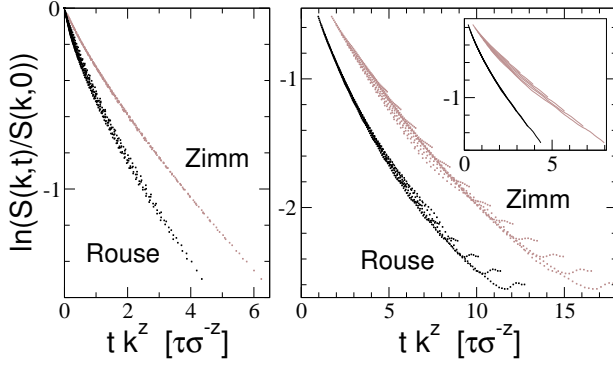


FIG. 3: Dynamic structure factor of the charged chain scaled with Zimm ( $z = 3$ , light circles) and Rouse ( $z = 3.5$ , black circles) for wavevectors  $0.2 < k < 0.5$  and time  $t < t_0 = 55$  (left) and  $t > t_0$  (right). The inset on the right shows data for large wavelengths,  $k < k_0 = 0.3$  at  $t_0 < t < t_{\text{zimm}} = 300$ , which exhibit Rouse scaling as already demonstrated in Fig. 2. The main graph shows the data for short wavelengths,  $k > k_0 = 0.3$  and time  $t_0 < t < 150$ .

tions are screened on large length scales. However, the screening is 'delayed' and not yet effective at early times  $t < t_0 = 55$ . A similar effect has been observed by Ahlrichs et al. in semidilute polymer melts<sup>10</sup>. In this case, the initial decay of  $S(k;t)$  was found to be governed by an unscreened diffusion tensor. Screening sets in as soon as chains interact with each other, i.e., mesh blobs have moved their own size. Beyond that time, chain parts cannot follow the flow and act as immobile obstacles that produce Darcy-type friction.

In our case, the phenomenon is similar, but the underlying physics is clearly different. The large reduction of the diffusion constant in the presence of charges ( $D_c < D_u$ ) suggests that the chain dynamics is mainly driven by electrostatics, like in electrophoresis, where hydrodynamic screening is also observed. However, the derivation of the screened Oseen tensor in electrophoresis relies crucially on the fact that the monomer and the surrounding ion cloud are subject to a homogeneous electrical field. Intrachain interactions produce inhomogeneous fields, thus the theory cannot be applied. Moreover, we need to explain the screening delay, i.e., the Zimm-Rouse crossover observed in our simulations.

To analyze the problem in more detail, we begin with investigating the time scales governing the dynamics of charge distributions in our system. To this end, we calculate the dynamic "charge structure factor"  $S_q(k;t) = \langle \tilde{I}_q(k;t) \tilde{I}_q(k;0) \rangle$  with  $\tilde{I}_q = \sum_i q_i e^{ik \cdot R_i}$ , where the sum  $i$  runs over all charged particles and  $q_i$  denotes their charge. The result is shown in Fig. 4 (left). In the simplest linearized dynamical mean-field theory, the charge distribution decays exponentially towards the Debye-Huckel distribution with the characteristic decay time  $\tau_D(k) = 1/k_B T (k^2 + \kappa_D^2)$ . In the simulations, the decay of  $S_q(k;t)$  is slightly slower and depends less on  $k$  (presumably due to the fact that the motion of the ions is

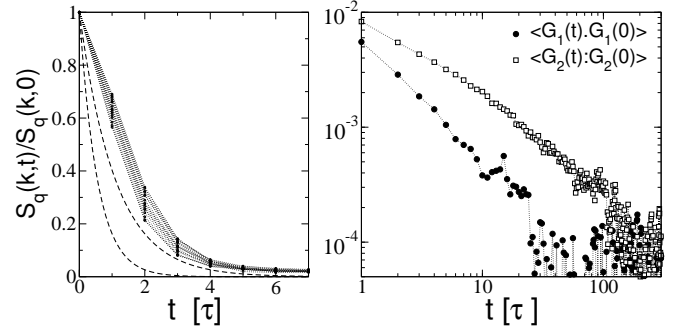


FIG. 4: Illustration of time scales governing the charged system. Left: dynamic charge structure factor in the range  $k_D < 1$ . Dashed lines show theoretically predicted exponential decay  $\exp(-t/\tau(k))$  (see text) for  $k = 0$  (upper curve) and  $k = 1/k_D$  (lower curve). Right: Autocorrelation function of  $G_1(t)$  and  $G_2(t)$  (see text for definitions). Here  $\bullet$  denotes dot product and  $\circ$  double-dot product (double contraction).

not yet diffusive on the time scale  $\tau_D$ . Nevertheless, the charge distribution has clearly relaxed on the time scale  $t_0$  of the Zimm-Rouse crossover. On this time scale, the ions follow the chain adiabatically.

We thus proceed to calculate the velocity field  $v$  generated by the chain in the Debye-Huckel and Stokes approximation. For simplicity, we neglect the finite diameter of monomers and ions. The chain is characterized by the positions  $R$  of the monomers and their central charge  $q$ . Each monomer charge generates a charge distribution  $\rho(r)$ , which in turn generates an electrostatic field  $E(r)$  and imparts a force field  $f_{el}(r) = \rho(r)E(r)$  to the uid. In addition, non-electrostatic interactions (e.g., bond interactions) between monomers and generate forces  $f(r)\delta(r - R)$  at  $r = R$ , which are also transmitted to the uid. Here  $r = R - R$  and  $\hat{r} = r/r$ .

We consider the limit  $k = 1/k_D$ , i.e., we focus on the length scale regime well above the Debye-Huckel screening length. After working out the theory, we obtain the velocity field  $v(k) = \exp(ik \cdot R) v^{(1)}(k)$ ,

$$v^{(1)}(k) = \frac{1}{k^2} \sum_n f_n + \frac{q q}{2} g \frac{r}{D} e^{ik \cdot r} (1 - \hat{k} \hat{k}) \hat{r} \quad (1)$$

with  $g(x) = e^x (x^2 - 2x - 1) = \hat{x}$  and  $\hat{k} = k/k_D$ , where  $\hat{k} \hat{k}$  denotes the tensor product. A derivation of this expression shall be given elsewhere. From Eq. (1), one readily calculates the flow velocity at the position of a monomer  $r$ ,  $v(R) = v^{(1)}(r)$ . The contributions  $v^{(1)}$  are conveniently expanded in multipoles. Here we quote only the monopole and dipole term

$$v_m^{(1)}(r) = \frac{1}{8} \sum_n f_n \frac{r}{r} + \frac{q q}{2} g \frac{r}{D} (1 + \hat{r} \hat{r}) \quad (2)$$

$$v_d^{(1)}(r) = \frac{1}{8} \frac{r}{r^3} \sum_n f_n \frac{q q}{2} g \frac{r}{D} r (3\hat{r} \hat{r} - 1) \quad (3)$$

The non-electrostatic interactions  $f$  between

monomers only contribute to the monopole term, Eq. (2). Inspecting the latter, one notices that it vanishes for locally straight chains, because contributions of vectors  $\mathbf{r}_0 = \mathbf{r}$ . For symmetry reasons, the time-averaged conformations of the chain have this property. Therefore, one might speculate that the monopole becomes small compared to the higher order multipoles on sufficiently large time scales. On the other hand, it is clear from Eq. (1) that all multipoles must vanish on time scales where the vectors  $\mathbf{r}$  are distributed isotropically. We thus need to compare the characteristic decay times for the monopole and the higher order multipoles quantitatively. To this end, we have evaluated the autocorrelation function of the vector  $G_1(t) = \langle \mathbf{q} \mathbf{q} \mathbf{g}(\mathbf{r} = \mathbf{r}_0) \rangle_t$ , which characterizes the monopole term, and that of the traceless part  $G_2(t)$  of the tensor  $\langle \mathbf{q} \mathbf{q} \mathbf{g}(\mathbf{r} = \mathbf{r}_0) \mathbf{r} \rangle_t$ , which characterizes the dipole term. Here  $\mathbf{r}_0$  was chosen to be the central monomer in the chain. The results are shown in Fig. 4 (right). For  $G_1$ , the decay is much faster than that for  $G_2$ . By the time  $t_0$  (55  $\tau$ ), the function  $\text{hbf} G_1(t) / G_1(0)$  has dropped by two orders of magnitude. This suggests that the dynamics of the chain is indeed governed by the higher order multipole interactions at later times. In the Stokes approximation, the latter vanish too, but much slower than the multipole term. If one includes nonlinear hydrodynamics, additional interactions come into play that presumably do not vanish at all. For example, the inhomogeneous velocity field created by the monomer in the vicinity of monomer  $i$  convects the ion cloud surrounding  $i$ . This contributes an effective additional force field in the vicinity of  $R$ , which in turn retroacts on  $i$ , leading to an induced hydrodynamic interaction that remains finite at all times.

Based on these considerations, we rationalize our simulation results as follows: On short time scales, the monopole term, Eq. (2) dominates, hydrodynamic inter-

actions are effective and lead to Zimm scaling. On longer time scales, time-averaged chains become locally straight and higher order terms take over. Zimm scaling is then replaced by Rouse scaling<sup>11</sup>. The relevant characteristic length scale for the process of local chain straightening is twice the maximal distance between interacting monomers  $\{$  in our case, roughly  $\approx 3.4$ , since the mean distance between charged monomers in the chain is roughly  $a_0 = 1.7$  and  $\langle r \rangle < a_0$ . This corresponds well with the observation that the Rouse scaling breaks down for large wave vectors with  $k < k_0 = 1/\langle r \rangle$ . It also explains why the crossover time  $t_0$  from Zimm to Rouse behavior does not seem to depend on the wavevector  $k$ .

To summarize, we have studied the dynamical behavior of polyelectrolytes in salt solution on time scales below the Zimm time. At very short times, they behave like regular self-avoiding chains that are subject to hydrodynamic interactions. In an intermediate time scale range between a microscopic crossover time and the Zimm time, however, the chain behaves like a Rouse chain, i.e., hydrodynamic interactions are effectively screened. These findings should have implications for the interpretation of various processes of biological and nanotechnological interest. Many dynamical processes where polyelectrolytes are involved, such as DNA translocation through pores or RNA folding etc. are driven by internal chain modes. Our results indicate that the influence of hydrodynamics on these processes might be much smaller than is commonly assumed. Theoretical models that neglect hydrodynamics may be closer to reality than more refined models that include hydrodynamics.

We thank Burkhard Dunweg and Ulf Schiller for enlightening discussions. This work was funded by the VW foundation. The simulations were carried out on supercomputers at the HLRS in Stuttgart, the NIC in Jülich, and the PC<sup>2</sup> cluster in Paderborn, using the freely available software package ESPResSo<sup>12</sup>.

- <sup>1</sup> M. Doi and S. F. Edwards, *The Theory of Polymer Dynamics*, University Press, Oxford (1986).
- <sup>2</sup> J.-L. Barrat and J.-F. Joanny, in *Polymeric Systems, Advances in Chemical Physics Vol. XCIV*, edited by I. Prigogine and A. Rice, J. Wiley & Sons, New York (1996).
- <sup>3</sup> E. Stellwagen, Y. Lu, and N. C. Stellwagen, *Biochemistry* 42, 11745 (2003).
- <sup>4</sup> G. S. Manning, *J. Phys. Chem.* 85, 1506 (1981).
- <sup>5</sup> K. Grass, U. Bohme, U. Scheler, H. Cottet, and C. Holm, *Phys. Rev. Lett.* 100, 096104 (2008).
- <sup>6</sup> S. Frank and R. G. Winkler, *Europhys. Lett.* 83, 38004 (2008).
- <sup>7</sup> P. Español and P. B. Warren, *Europhys. Lett.* 30, 191

- (1995).
- <sup>8</sup> P. Ahlrichs and B. Dunweg, *J. Chem. Phys.* 111, 8225 (1999).
- <sup>9</sup> B. Dunweg and K. Kremer, *J. Chem. Phys.* 99, 6983 (1993).
- <sup>10</sup> P. Ahlrichs, R. Everaers, and B. Dunweg, *Phys. Rev. E* 64, 040501(R) (2001).
- <sup>11</sup> Rouse scaling is expected for hydrodynamic interactions decaying faster than  $r^{-1}$ .
- <sup>12</sup> A. A. Mold, B. A. Mann, H.-J. Limbach, and C. Holm, *Comp. Phys. Comm.* 174, 704 (2005).